SJESC
Souf Journal of Engineering and Sustainable Chemistry
*Souf Journal of Engineering and Sustainable Chemistry (SJESC)*
*ISSN:3088-831X*
*2026. Vol. 2, N°. 1, 010-025*
*Journal homepage: https://sjescjournal.com*

*Article*

# Sorption Potential of *Piliostigma Reticulatum* Biomass Towards Bromophenol Blue Removal from Aqueous Solution

**Sali Mouhamadou[1, 2 *], Bouba Talami[2], Jourdin Gongwala[3], Djouleyatou Yaya Gue-Yre[2], Mamat Ousman Bouza[2], Sadou Dalhatou[2], Massai Harouna[1]**

[1]Department of Chemistry, Faculty of Science, University of Garoua, Garoua Cameroon
[2]Department of Chemistry, Faculty of Science, University of Maroua, Maroua Cameroon
[3]Department of Chemistry, Higher Teacher Training College, University of Maroua, Maroua Cameroon
*****Correspondence: mouhamadouahmedsali@yahoo.com

**Article Information**

**Article History**
Received : 27-03-2026
Revised : 25-05-2026
Accepted : 31-05-2026

**Keywords:** Kinetics, Adsorption, Bromophenol Blue, Isotherm, *Piliostigma eticulatum.*

**Abstract**

Eco-friendly biomaterial was prepared from piliostigma fruits wild bio-waste. The structure, morphology, chemical composition and crystalline phase of the prepared biosorbent was systematically characterise using some modern techniques like Fourier transform infrared spectroscopy (FTIR), Scanning electron microscopy (SEM), X-ray fluorescence spectrophotometry fundamental parameters (XRS-FP) and X-ray Diffraction (XRD). Piliostigma biomaterial was applied in the removal of Bromophenol Blue (BPB) dye from aqueous solution using batch mode under optimum conditions. The optimum BPB dye adsorbed was 13.7 mg/g at pH 6 for a contact time of 60 min with adsorbent dose of 0.01 and a concentration of 40 mg/L. the adsorptive removal process followed pseudo-second order kinetic with high $R^2$= 0.98, suitable uptake capacity $q_e$= 5.27 mg/g and fitted best the Dubinin Radushkevich equilibrium isotherm model that correlate chemisorption mechanism with low energy E= 0.364 kJ/mol, $R^2$= 0.97 and $q_e$= 14.02 mg/g. these results suggest that prepared biosorbent is a new promising material that have potential applications in the treatment of effluent containing dye pollutant.

## 1. Introduction

Numerous biomaterials have been used to improve water quality in recent years. One of the main causes of pollution of expanses of water is industrial waste, which has a negative impact on the environment[1]. Organic dyes represent effective chemical hazard encountered in our environment as organic pollutants[2]. About 1.6 million tons of dyes are being manufactured annually; 10-15% of which are being discarded in the form of unprocessed wastewater effluent into the aquatic systems[3] .Bromophenol blue is a non-biodegradable synthetic hazardous dye which has wide applications as colour marker in labs, as acid-base indicator and for agarose gel electrophoresis; along with applications in drug, cosmetics, textile and printing ink industries [4]. Bromophenols have shown serious impact on the ecosystem due to their genotoxic, mutagenic and carcinogenic properties[5] . Therefore, the treatment of effluent containing such dye has great interest to limit their harmful impacts. Relevant research investigations have focused on the removal of dyes such as methylene blue, congo red[6], crystal [7], methyl orange, rhodamine B [8] and direct red 80 [9], with only few reports on bromophenol blue [6]. Bromophenol blue (BPB), a widely used dye, can easily migrate through aquifers and generate widespread pollution of surface waters owing to highly solubility and

solubility [10]. Hence, the removal of BPB dye from industrial wastewater through a simple and eco-friendly process should be given significant attention.

Importance of wastewater quality find interest with application of various physicochemical treatment methods such as coagulation, chemical oxidation [11], photodegradation, nanofiltration [12], bioremediation, flocculation, ozonation[13], photocatalysis [14]and adsorption[15], [16] .However, most of these processes are capital intensive, complicated and required more chemicals. The adsorption method of pollutants onto biomaterials, known as biosorption is the preferred process, due to its simplicity, low cost, effectiveness, biodegradability and reusability[6], [17] . Several biomasses have been used for dye removal such as rice husk, orange peels, corncob, cotton waste, sugarcane bagasse, just to mention few[18]. Based on the concept of Green Chemistry and in the framework of circular economy, agricultural biomass waste are potential candidates for the development of materials with adsorptive properties[19]. Among them, *Piliostigma reticulatum* fruits is one of the most important wild solid wastes which represents a potential and eco-friendly biomass that can be use in water treatment technology.

To the best of authors' literature knowledge, there are no studies on the use of piliostigma biomass for the removal of BPB and its physicochemical characterisation. This study reports for the first time, *piliostigma reticulatum* characteristics and investigate the adsorption capability of BPB. Efficacy of piliostigma biomass over dye retention has been investigated at varied key operational parameters such as contact time, adsorbent dose, pH and concentration. Equilibrium modelling of isotherms and kinetics were illustrated to analyse the adsorption data in other to propose adsorption mechanism and phenomenon.

## 2. Material and Methods

### *2.1. Reagents*

The dye solid powder of BPB was purchased from REACTIFS RAL (Paris, France). The general characteristics and structure of BPB are presented in Table 1. Stock solution of 500 mg/L was prepared using 0.5 g in 0.5 L of osmotic water and the derived solutions with desired concentrations were obtained via dilution process. HCl and NaOH diluted solutions were used to adjust the pH values. All chemicals were of analytical grade and used without any further purification.

**Table 1.** Chemical characteristics and structure of BPB dye.

| **Characteristic** | **Bromophenol Blue (BPB)** |
|---|---|
| Molecular Structure | 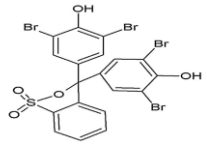 |
| Chemical formula | $C_{19}H_{10}Br_4O_5S$ |
| Molecular weight (g/mol) | 669.96 |
| $\lambda_{max}$ (nm) | 592 |

### *2.2. Preparation of Biomaterial*

The biomaterial (piliostigma fruit) used in the present study were collected from pont palais hills, Mayo-Oulo, North region of Cameroon. The fruits were thoroughly cleaned with distilled water and dry in air oven at 105°C for 24h. The dry fruits were crushed using a grinder and sieved to get particles less than 315 µm. the obtained biomass was used for characterisation and adsorption studies of BPB dye.

### *2.3. Characterisations*

The elemental and chemical composition of the biomaterial was determined using X-ray fluorescence spectrometry Fundamental Parameter (XRS-FP) while the crystallinity was examined by X-ray diffraction. The diffraction patterns were recorded from 5 to 80°. The biomass powder was structurally and morphologically characterised in a VEGA TESCAN high resolution scanning electron microscopy (SEM). The existence of functional groups on the surface of the materials was analysed by Fourier transform infrared spectrophotometry (FTIR) using Perkin Elmer apparatus at the wavenumber ranging between 4000 $cm^{-1}$ and 400 $cm^{-1}$.

### *2.4. Batch adsorption experiments*

Adsorption experiments were conducted in batch mode where at each run, 20 mL of BPB solution with required concentration was added in 50 mL Erlenmeyer flask and agitated on magnetic stirrer (VWR Stirrer) for required time at constant speed of 600 rpm. Some key operational parameters such as contact time (10-80 min), adsorbent dose (0.01-0.08 g), initial pH (4-10) and BPB concentration (15-40 ppm) were studied. After each experiment completed, the liquid phase was separated from solid phase by filtration using a microfilter (0.45 µm). The initial and residual dye concentration were measured using a UV spectrophotometer (SHIMADZU UV-1800, USA 70387) at maximal wavelength value of 592 nm. The adsorbed quantity of BPB per gram of adsorbent, $q_e$ (mg/g) were calculated using equation (1).

$$q_{e/t} = \frac{(C_o - C_{e/t})V}{m} \quad (1)$$

Where $C_o$ and $C_{e/t}$ are initial and equilibrium concentration or at specific time of BPB dye solution (mg/L) respectively, $V$ is the total volume of BPB dye solution (L) and $m$ stands for the mass of adsorbent (g). The removal Yield were also calculated using equation (2).

$$R(\%) = \frac{(C_o - C_e)}{C_o} x100 \quad (2)$$

## 3. Results and Discussion

### *3.1. Physicochemical characterisations*

#### *3.1.1. X-ray Diffraction (XRD) analysis*

XRD analysis was applied to detect the level of crystallinity of piliostigma biomaterial and pattern is shown in Figure 1. The peak at 2Θ= 11.46° and 22.66° correspond to peak of

crystalline cellulose[20].The peak of 22.66° was defined as a crystallographic plane of cellulose[21]. Furthermore, these results are in agreement with the report of Satyanarayan et al. [22] when they characterised Canadian biomass for alternative renewable biofuel.

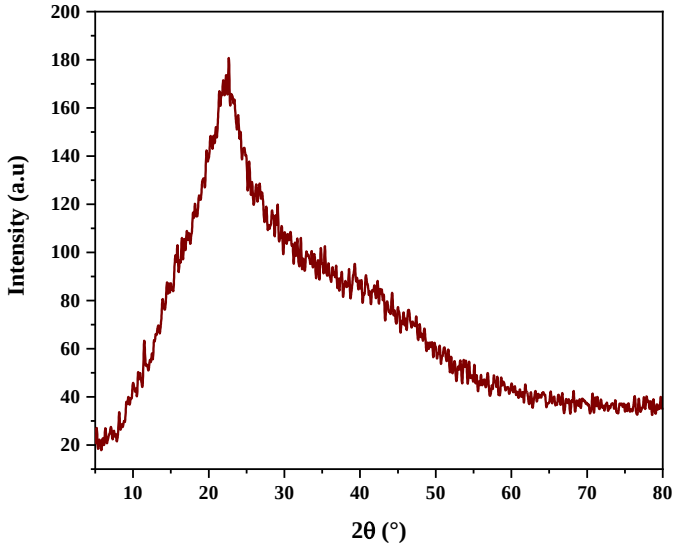


**Fig. 1** XRD spectra of piliostigma biomaterial.

### *3.1.2. Scanning electron microscopy (SEM)*

The SEM was performed to study the microstructure of different sections of piliostigma biomaterial sample with different magnifications. According to the detail's morphology aspects, the obtained micrograph of piliostigma biomass shows a gentle surface with no pores as shown in Figure 2(a and b). The biomass used in this study had almost negligible pores and this observed trend was in agreement with the results obtained by Sahoo et al.[21]. Furthermore, it contains a uniform shape and size and highly agglomerated, this may be attributed to the fact that no treatment of the biomass was involved.

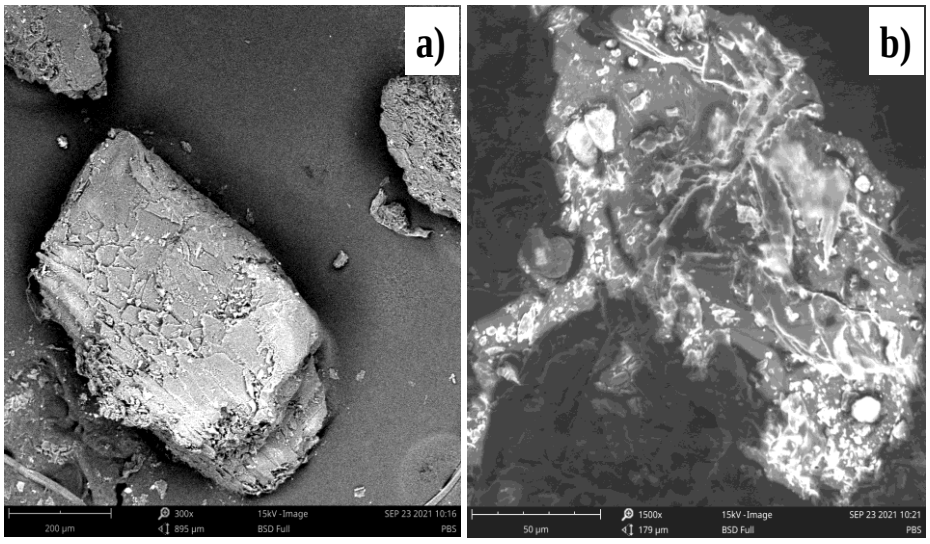


**Fig. 2** SEM spectra of piliostigma biomaterial.

### *3.1.3. Fourier transform infrared spectrophotometry (FTIR)*

FTIR spectrum of pristine piliostigma biomaterial is shown in Figure 3. The spectra is typical of lignocellulosic biomass and display a series of very sharp absorption peaks due to the crystallinity of the samples. As indicated, OH stretching vibration is depicted at 3277 $cm^{-1}$ due to the presence of carboxylic acid, alcohol and moisture[20] while C-H stretching was observed at 2927 $cm^{-1}$ [6]since no carbonisation and/or activation of piliostigma biomaterial was involved. Adsorptions at 1610 $cm^{-1}$, 1025 $cm^{-1}$ corresponded to C=O, C-O functional groups signifying the existence of ketones, ester, carboxylic acids and aldehydes[21], [23]. The wide band at 2160-2020 $cm^{-1}$ is ascribed to C=C of alkenes[24]. The peak at 1448 $cm^{-1}$ presented the C-H vibrations indicating alkanes [25] while the peak at 1248 $cm^{-1}$ were attributed to C=C of aromatic group. The presence of several functional group on the surface of piliostigma biomass as identify by FTIR indicates the potential of this biomaterial to interact with pollutants (BPB in solution).

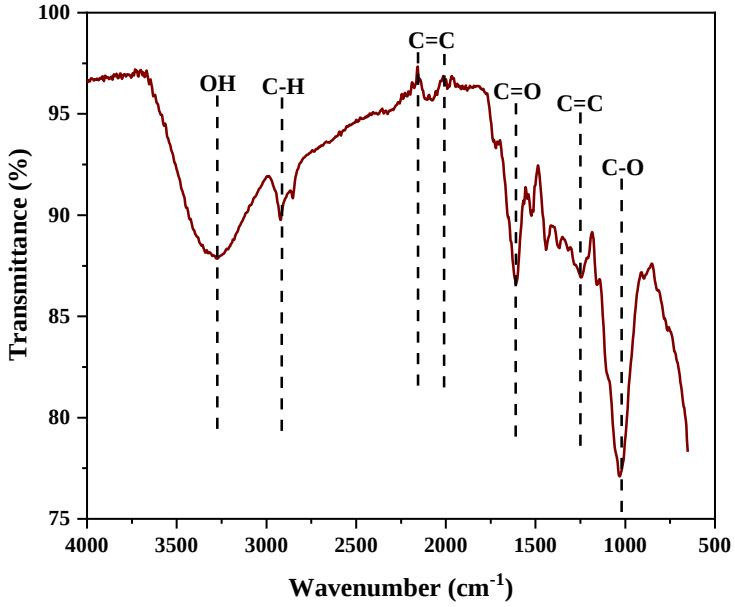


**Fig. 3** FTIR spectra of piliostigma biomaterial.

### *3.1.4. X-ray fluorescence spectrometry fundamental parameters (XRS-FP)*

To better understand the contents in term of chemical and elemental composition of piliostigma biomaterial, XRS-FP was performed to identify inorganic elements and mineral matters. In the present study, for most part, piliostigma biomass implied maximum percentage of O, Ca, K, Mg, Al, Cl and minor percentage of Si, S, Fe as tabulated in Table 2. Similar results were reported by Sahoo et al. [26] when the characterised non-edible lignocellulosic biomass to elucidate their biofuel production potential. These metalloid elements were also found by Oo et al.[27]in the forest and sugarcane leaf biomass.

**Table 2.** Elemental composition of piliostigma biomaterial.

| Element | O | Mg | Al | Si | S | Cl | K | Ca | Fe | Others |
|---|---|---|---|---|---|---|---|---|---|---|
| **Concentration(%)** | 32.302 | 15.194 | 4.816 | 2.050 | 1.636 | 3.333 | 17.837 | 19.844 | 1.187 | 1.8 |

Piliostigma biomaterial exhibited high content of CaO (27.80%) followed by MgO (25.20%), $K_2O$ (21.50%), $Al_2O_3$ (9.10%), $SiO_2$ (4.39%), $SO_3$ (4.09%), Cl (3.30%), $Fe_2O_3$ (1.68%), $P_2O_5$ (1.40%) and other components as summarized in Table 3. These results was very similar to other reported biomass such as rice husk, cotton stalk, wheat straw, corn stover, sorghum stalk, corn cob…etc. Additionally, the oxides in the piliostigma biomass can be divided into acidic oxides ($SiO_2$, $Al_2O_3$, $SO_3$, $P_2O_5$ etc.) and basic oxides (CaO, MgO, $K_2O$, $Fe_2O_3$) according to their acidic and basic capacities[28] .

As shown in Table 3, CaO, MgO, $K_2O$ are predominant in the biomaterial with a total content of more than 70 wt%. The results suggest that these elements can facilitate the interaction between pollutants and the biomaterial trough adsorption process.

**Table 3.** Chemical components of piliostigma biomaterial.

| Component | $SiO_2$ | MgO | $Al_2O_3$ | $Fe_2O_3$ | $SO_3$ | Cl | $K_2O$ | CaO | $P_2O_5$ | Others |
|---|---|---|---|---|---|---|---|---|---|---|
| **Concentration (%)** | 4.39 | 25.20 | 9.10 | 1.68 | 4.09 | 3.30 | 21.50 | 27.80 | 1.40 | 1.54 |

### *3.2. Adsorption tests results*

#### *3.2.1. Effect of contact time*

Equilibrium time is one of the most important parameters in designing the efficiency of an adsorbent. It informs about the removal rates of pollutants in adsorption process. It is known that high removal at short contact time revealed that film diffusion is a controlling reaction step while high removal at long contact time indicates that intraparticle diffusion may be the controlling step[29]. The adsorption of BPB dye onto piliostigma biomaterial at initial concentration of 15 ppm (pH 4.35) was studied as function of contact time to reach the adsorption equilibrium time (see Figure 4). The results reveal that about 38.5% of BPB was adsorbed with the maximum of uptake capacity of 5.77 mg/g at an equilibrium time of 60 min. this result indicates that the intraparticle diffusion contribute to the rate determining step. El-Gamal et al.[29] observed similar phenomenon when removing methyl orange and BPB in aqueous solution with Sorel's cement.

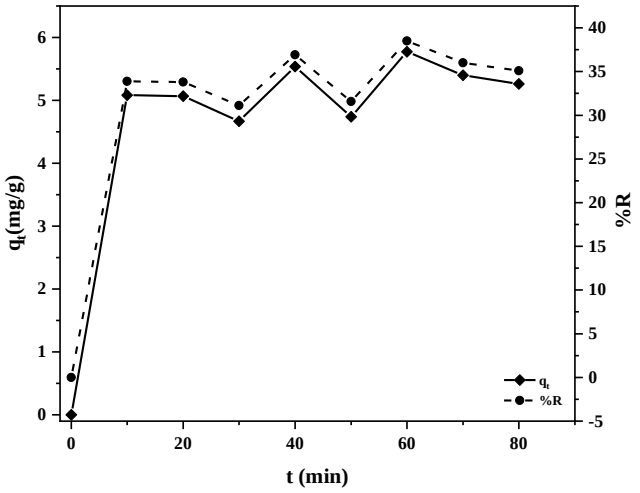


**Fig.4** Effect of contact time.

#### *3.2.2. Effect of adsorbent dose*

Catalyst dose is considered as a key factor for choosing solid when dealing with the removal of organic wastes. A higher uptake quantity of pollutants in a short mass and establishment of equilibrium means high efficiency of the solid towards the removal of organic pollutants. This shows its ability for quantitative removal of BPB of initial concentration of 15 ppm and fixed pH of 4.35. The obvious trend of increase in removal percentage and a decrease in adsorption adsorbed capacity is shown with the adding of piliostigma biomaterial dose (see Figure 5). Increment of removal percentage of BPB by raising the mass of catalyst is observed and reach a percentage of 59.31% with 0.08 g of piliostigma biomaterial from Figure 5. However, a decrease of adsorbed amount is shown with the addition of adsorbent dose. The best uptake capacity is obtained with a catalyst dose of 0.01 g. these results implemented that rapid increase of adsorption percentage with raising adsorbent dose is due to the important driving force it causes towards BPB, availability and more active sites. This means there is lower dye molecules in vacant site that leads to higher migration and diffusion of BPB molecules. The higher uptake quantity of pollutants at lower mass is attributed to the best dispersion of adsorbent in the medium with absence of formation of aggregate that masked some active site. This trend is in agreement with the report of Ghaiedi et al.[30] when they removed BPB in aqueous solution using activated carbon from Astragalus bisulcatus tree.

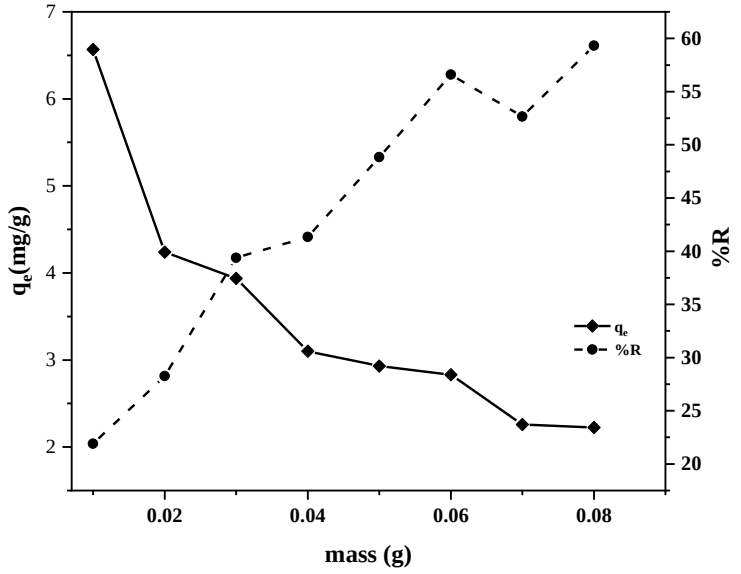


**Fig. 5** Effect of adsorbent dosage.

### *3.2.3. Effect of pH*

pH is the second most important key operational parameter that imposes several significant effects on the surface of adsorbents as well as pollutant solution in the adsorption process. Electrostatic interaction is closely related to pH which determines the form of dye chemical specification, solubility and modify by ionisation some functional groups, the charge of the surface of adsorbent. As illustrated in Figure 6, adsorption capacity and removal percentage of BPB on the piliostigma biomaterial decrease 9.78 to -0.6 mg/g and 32.62 to -2.1 % gradually with increase of pH from 6 to 12. This trend shows that lower pH (in this case neutral pH) of solution is favourable for BPB adsorption on piliostigma biomaterial due to the anionic nature of the dye. Similar results of steady decrease of BPB adsorption with raising pH was also cited

in literature[6], [30] . Piliostigma biomaterial has lower adsorption capacity of BPB at high pH can be ascribe to electrostatic repulsion between negative form of BPB in solution and the negative charge of the surface while we observe high uptake capacity of BPB at lower pH which signifies electrostatic attraction between BPB and the positive surface sites of the biomaterial[31]. This result establishes the fact that BPB adsorption is favourable at neutral pH which occurs in real industrial wastewater.

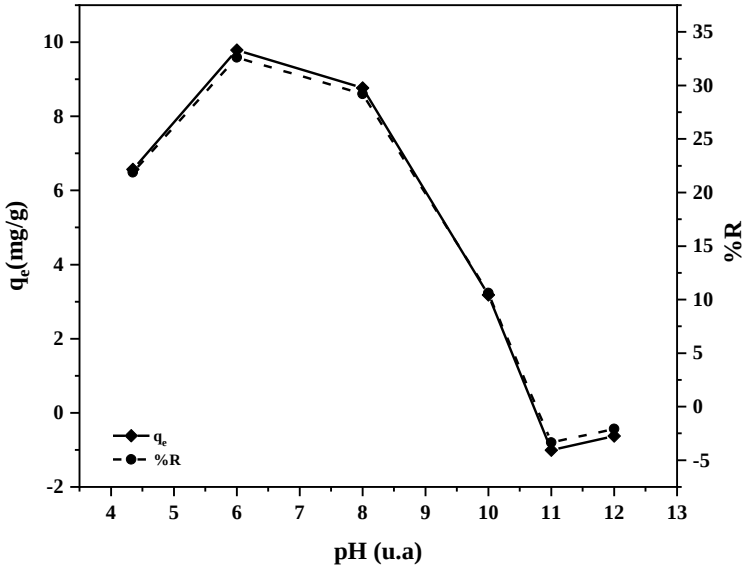


**Fig. 6** Effect of pH.

### *3.2.4. Effect of dye concentration*

A given mass of piliostigma biomaterial can adsorb only fixed amount of BPB, that's why the initial dye concentration plays an important role and provides an essential driving force for mass transfer between the adsorbate and solid phases in the adsorption process. The effect of initial concentrations on adsorption of BPB on piliostigma biomaterial was studied. As evident from the results depicted in Figure 7, the uptake capacity raised from 6.96 to 13.7 mg/g while a significant decreased in removal percentage (34.82 to 17.12%) that emerged from total occupation and saturation of surface-active sites upon increasing dye concentration. the higher absorbed quantity is ascribed to greater interaction of BPB dye with active groups on the surface of the biomaterial, resulting from higher abundance of pollutants that occupied the maximum sites. However, we noticed that simultaneous decreased of removal percentage could be due to the fact that, the considered mass become saturated at higher concentrations, leaving more residual BPB behind in solution. The results agree with the observations of other authors in literature[6, 32].

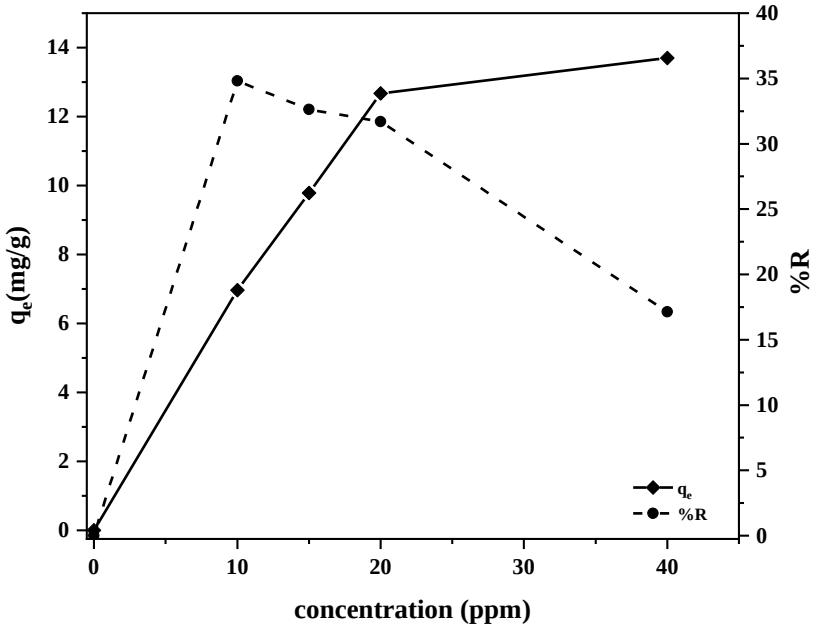


**Fig. 7** Effect of initial BPB dye concentration.

### *3.3. Kinetics modelling analysis*

Adsorption kinetics determine how fast BPB is removed from solution using piliostigma biomaterial. It is an important tool for economic reason, as well in designing adsorption system. Kinetics study is a vital aspect that helps for understanding the reaction mechanism of BPB dye adsorption. Best fitting of experimental data in this present trend was verified through several reaction control models corresponding to these four: pseudo-first order, pseudo-second order, Elovich and Intraparticle diffusion. All equations are summarised in Table 4 below.

**Table 4.** Linear and Nonlinear kinetics model equations.

| Kinetic models | Linear equations | Non-linear equations | References |
|---|---|---|---|
| Pseudo first order | $\ln(q_e - q_t) = \ln q_e - K_1 t$ | $q_t = q_e[1 - \exp(-K_1 t)]$ | [33] |
| Pseudo second order | $\frac{t}{q_t} = \frac{1}{K_2 q_e^2} + \frac{t}{q_e}$ | $q_t = \frac{q_e^2 K_2 t}{1 + q_e K_2 t}$ | [34] |
| Elovich | $q_t = \frac{1}{\beta}\ln(\alpha\beta) + \frac{1}{\beta} lnt$ | $q_t = \frac{1}{\beta}\ln(1 + \alpha\beta t)$ | [33] |
| Intraparticle diffusion | $q_t = k_{int}\sqrt{t} + c$ | $q_t = k_{int}\sqrt{t} + c$ | [34] |

where $q_t$ and $q_e$ (mg.g$^{-1}$) is the amount of adsorbed at any time $t$ and at equilibrium respectively. $k_1$ (min$^{-1}$) is the rate constant of pseudo first order and $k_2$ (g.mg$^{-1}$min$^{-1}$) is the rate constant of pseudo-second order of the adsorption process. $k_{int}$ is the intraparticle diffusion rate constant (mg.g$^{-1}$.min$^{-1/2}$) and c represents the value of the thickness of the boundary layer (mg.g$^{-1}$). α refers to the initial adsorption rate (mg(g.min)$^{-1}$) and β is related to the activation energy for chemisorption (g.mg$^{-1}$).

Kinetic parameters derived from fitting adsorption data of BPB dye are collected in Table 5 and the representative nonlinear plots are presented in Figure 8. As implemented, the

adsorption of BPB on piliostigma biomaterial showed good nonlinear plot of pseudo-second order and intraparticle diffusion rather than pseudo-first order and Elovich. The $R^2$ (0.98) value is closer to 1 and the calculated uptake capacity ($q_{ecal}$) of pseudo-second order matched well with the one of experimental data ($q_{exp}$). These results lead to the conclusion of higher affinity and fast bonding of BPB molecules to the surface of piliostigma biomaterial. In addition, the rate constant $K_2$ is higher than others indicating faster equilibrium of BPB uptake desired in adsorption system for practical application in industrial wastewater treatment. The highest value of thickness shows that the intraparticle diffusion contribute to the rate determining step as provided by high contact time. The results of this trend suggest that, adsorption process follows chemisorption mechanism as can be confirmed by FTIR with functional groups, XRS-FP with various components that can provided electrostatic interaction and SEM which shows lower presence of pores.

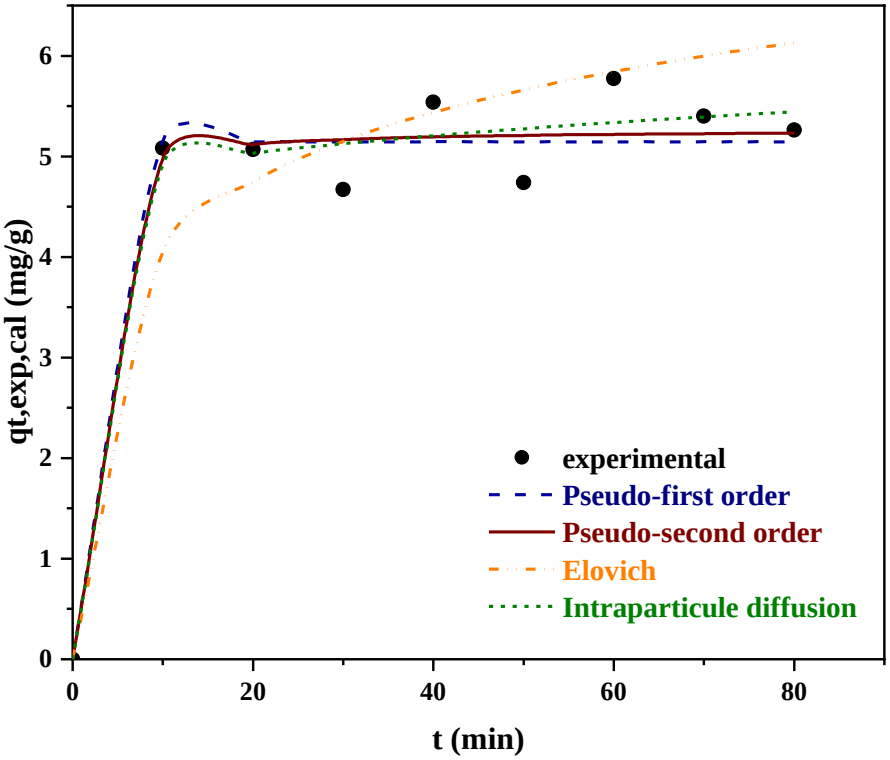


**Fig. 8** Nonlinear plot of kinetic models.

**Table 5.** Calculated parameters for kinetics of BPB dye adsorption.

| Material | $q_{exp}$ | pseudo first order | | | pseudo second order | | | Intraparticle diffusion | | | Elovich | | |
|---|---|---|---|---|---|---|---|---|---|---|---|---|---|
| | | $R^2$ | $q_m$ | $k_1$ | $R^2$ | $q_m$ | $k_2$ | $R^2$ | $k_3$ | c | $R^2$ | Ɓ | α |
| Biomass | 5.77 | 0.12 | 5.14 | 150.49 | 0.98 | 5.27 | 0.32 | 0.16 | 0.09 | 4.62 | 0.13 | 14.02 | $3.64.10^{25}$ |

### *3.4. Equilibrium modelling of isotherms analysis*

Adsorption isotherm modelling represents mathematical relation of uptake capacity target per gram of catalyst to equilibrium concentration at fixed time and temperature. It revealed strong knowledge about surface properties of adsorbent and BPB dye removal mechanism. The equilibrium data of BPB dye molecules are analysed by them to Langmuir, Freundlich and

Dubining Raduskevich model. The regression equation of both models are collected in Table 6.

**Table 6.** Linear and Nonlinear isotherm models equations.

| Models | Linear equation | Non-linear equation | References |
|---|---|---|---|
| **Langmuir** | $\frac{1}{q_e} = \frac{1}{q_m K Ce} + \frac{1}{q_m}$ | $q_e = \frac{q_m K_L C_e}{1 + K_L C_e}$ <br> $R_L = \frac{1}{1 + K_L C_0}$ | [35] |
| **Freundlich** | $\ln q_e = lnK_F + \frac{1}{n} lnC_e$ | $q_e = k_f c_e^{1/n}$ | [36] |
| **Dubinin-Radushkevich** | $lnq_e = \ln q_{max} - \beta\varepsilon^2$ | $q_e = q_{max} exp\left[\frac{RTln(1+\frac{1}{C_e}))^2}{-2E_a^2}\right]$ <br> $E = (2\beta)^{-1/2}$ | [37] |

The Langmuir model assumes a monolayer adsorption mechanism where the adsorbent had fixed number of active sites of similar activation energy and affinity toward the adsorbate. In this model, the steric limitation between the adjacent adsorbate species was ignored[35] . $q_{max}$ and $K_L$ are the Langmuir constants which are related to the adsorption capacity.
The Freundlich adsorption isotherm suggest a multilayer adsorption mechanism where various sites with different adsorption energies are involved[36]. It is assumed that the heterogeneous surface of adsorbent exhibits non-uniform distribution of adsorption heat instead of exponential decrease upon the end of adsorption process. $K_F$ and $n$ are the Freundlich constants which are related to adsorption capacity and intensity.

The Dubinin-Radushkevich model is generally used for adsorption mechanism with a Gaussian energy distribution onto heterogeneous surface. Through this isotherm, it is possible to analyse more deeply the type of adsorption [37].

The related non-linear plots corresponding to these isotherms model are presented in Figure 9 and the calculated parameters are collected in Table 7. As shown in Figure 9 the Dubinin-Radushkevich isotherm fitted best the experimental data as depicted by the highest $R^2$(0.97) and the calculated amount adsorbed ($q_{e,cal}$= 14.02) is more closer to the experimental value ($q_{e,exp}$= 13.70) than Langmuir and Freundlich isotherm model. The n constant of Freundlich model exhibited high affinity of the BPB molecules with the piliostigma biomaterial that is ascribed to high electrostatic interaction. The highest value of $K_f$ indicates multilayer binding of BPB onto heterogeneous surface of piliostigma biomass attributed to organic and inorganic components presence on the surface of the adsorbent as confirmed by the results of FTIR and XRS-FP. The dimensionless constant of Langmuir $R_l$ (0.17) implemented a favourable adsorption of BPB[38] onto piliostigma biomaterial. The adsorbed quantity of piliostigma biomaterial was compared with other adsorbents applied previously for the adsorption of BPB dye, as presented in Table 8.

Although the prepared biomaterial in this trend implemented lower adsorbed amount compare to numerous adsorbents in literature, it adsorption is much higher than MApe, MApe-

Mt (6.04 and 8.12 mg/g) [6], $Fe_3O_4$-CuO-AC (0.088 mg/g)[39], ZnO nanoparticles (3.24 mg/g)[40]. Furthermore, the prepared biomaterial offers the possibility to proceed at pH 6 which is suitable for industrial real wastewater. The simple, abundant and eco-friendly nature of the prepared biomaterial would be it main advantages for practical applications.

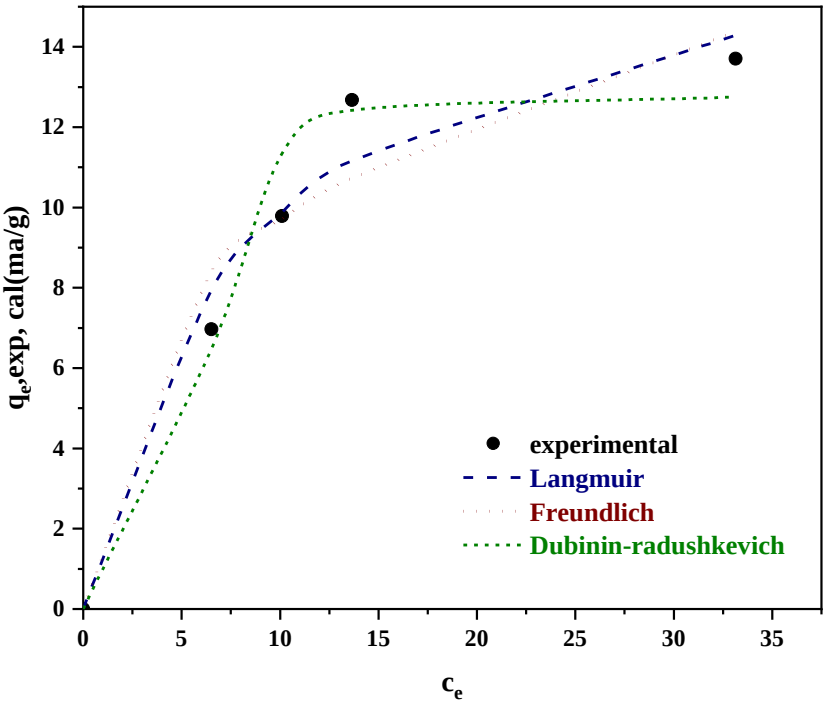


**Fig. 9** Nonlinear plot of isotherm models.

**Table 7.** Calculated parameters for isotherms of BPB dye adsorption.

| Material | $q_{exp}$ | Langmuir | | | | Freundlich | | | Dubining Raduskevich | | | |
|---|---|---|---|---|---|---|---|---|---|---|---|---|
| | | $q_m$ | $k_L$ | $R_L$ | $R^2$ | $K_f$ | n | $R^2$ | $q_m$ | B | E | $R^2$ |
| **Biomass** | 13.70 | 17.76 | 0.12 | 0.17 | 0.92 | 4.51 | 3.02 | 0.79 | 14.02 | 3.77E-06 | 0.364 | 0.97 |

**Table 8.** Comparative table of operational parameters and adsorption capacities for the removal of BPB dye by other alternative adsorbents.

| Catalyst | pH | Dosage (g) | Concentration (mg/L) | Time (min) | $q_e$ (mg/g) | References |
|---|---|---|---|---|---|---|
| MApe | 4.0 | 0.100 | 50 | 240 | 6.0400 | [6] |
| MApe-Mt | 4.0 | 0.100 | 50 | 240 | 8.1200 | |
| $Fe_3O_4$-CuO-AC | 5.3 | 0.100 | 10 | 120 | 0.0886 | [39] |
| $CoFe_2O_4$ | 6.5 | 0.400 | 20 | 120 | / | [12] |
| Activated Carbon | 1.0 | 1.000 | 10 | 50 | 23.450 | [30] |
| Sorel's cement nanoparticles | 8.3 | 0.250 | 25.14 | 90 | 16.390 | [29] |
| Chitin nanoparticles | 6.0 | 0.015 | 15 | 50 | 22.720 | [41] |
| Graphene Oxide | 7.0 | 0.010 | 15 | 10 | 17.940 | [42] |
| PAN nanofibers | 6.0 | 0.035 | 25 | 240 | 42.017 | [43] |
| PAN-CD nanofibers | 6.0 | 0.035 | 25 | 240 | 79.365 | |

| | | | | | | |
|---|---|---|---|---|---|---|
| RAL | 3.0 | 0.010 | 100 | 60 | 365.36 | |
| ALB | 3.0 | 0.010 | 100 | 60 | 535.65 | [44] |
| CAL | 3.0 | 0.010 | 100 | 60 | 730.46 | |
| ZF | 6.0 | 0.500 | 5 | 60 | 10.790 | [45] |
| NZF | 6.0 | 0.500 | 5 | 60 | 16.170 | |
| ZnO nanoparticles | 4.0 | 0.100 | 50 | 180 | 3.2400 | [46] |
| Hermetia biosorbent | 4.0 | 0.020 | 200 | 20 | 192.00 | [47] |
| Piliostigma biomaterial | 6.0 | 0.010 | 40 | 60 | 13.700 | This study |

## Conclusion

Being a useless and abundantly available wild bio-waste, *piliostigma reticulatum* fruits can be used as an eco-friendly and environmentally biosorbent for wastewater treatment. Piliostigma biomaterial was efficient in the removal of bromophenol blue dye as successfully demonstrated by adsorption experiment design and characterisation techniques that provided information on organic and inorganic composition (FTIR, XRS-FP), morphology (SEM) and crystallographic view (XRD) of the material. The best removal results obtained from key operational parameters were at pH 6 with 0.01g of biosorbent and BPB dye concentration of 40 mg/L for a contact time of 60 min. The pseudo-second order kinetic fitted best the experimental data at equilibrium time with an uptake capacity similar to the calculated value ($q_{exp}$ =5.77 mg/g and $q_{ecal}$ =5.27 mg/g) and higher correlation coefficient ($R^2$= 0.98). The Dubinin-Radushkevich equilibrium isotherm fitted adequately the experimental results whose adsorption maximum is 14.02 mg/g compare to 13.70 mg/g. these results revealed that, the interaction between the adsorbent and BPB dye follows chemisorption process as can be seen from low adsorption energy (0.364 kJ/mol). Piliostigma biomaterial presents a compatible performance toward removal of BPB dye event if it has affinity with other materials in literature. Piliostigma biomaterial differs from others because it is easy to prepare since no chemical reagent was involved, abundant, available and low cost. Therefore, its characteristics and qualities make it a suitable solid as a potential technology implemented on wastewater scale for the removal of pollutants such as BPB dye.

**Acknowledgment**

The authors thank the Laboratory of Chemistry of the faculty of Science of the University of Maroua for providing lab facilities.

**Funding**

This research received no external funding

**Ethical Statement**

This research does not contain any studies with human or animal subjects performed by any of the authors

**Data Availability Statement**

Not Applicable

**Conflicts of Interest**

The authors declare no conflicts of interest

## References


[1] P. Szołdra, M. Frąc, and W. Pichór, "Effect of sol composition on the properties of TiO2 powders obtained by the sol-gel method," *Powder Technol.*, vol. 387, pp. 261–269, 2021.

[2] A. A. El-Zahhar, N. S. Awwad, and E. E. El-Katori, "Removal of bromophenol blue dye from industrial waste water by synthesizing polymer-clay composite," *J. Mol. Liq.*, vol. 199, pp. 454–461, 2014.

[3] C. Patra, E. Suganya, S. Sivaprakasam, G. Krishnamoorthy, and S. Narayanasamy, "A detailed insight on fabricated porous chitosan in eliminating synthetic anionic dyes from single and multi-adsorptive systems with related studies," *Chemosphere*, vol. 281, p. 130706, 2021.

[4] H. Mazaheri, M. Ghaedi, A. Asfaram, and S. Hajati, "Performance of CuS nanoparticle loaded on activated carbon in the adsorption of methylene blue and bromophenol blue dyes in binary aqueous solutions: using ultrasound power and optimization by central composite design," *J. Mol. Liq.*, vol. 219, pp. 667–676, 2016.

[5] S. Naraginti and Y.-C. Yong, "Enhanced detoxification of p-bromophenol by novel Zr/Ag-TiO2@ rGO ternary composite: Degradation kinetics and phytotoxicity evolution studies," *Ecotoxicol. Environ. Saf.*, vol. 170, pp. 355–362, 2019.

[6] K. G. Akpomie and J. Conradie, "Efficient synthesis of magnetic nanoparticle-Musa acuminata peel composite for the adsorption of anionic dye," *Arabian Journal of Chemistry*, vol. 13, no. 9, pp. 7115–7131, 2020.

[7] T. Sansenya *et al.*, "Hydrothermal synthesis of ZnO photocatalyst for detoxification of anionic azo dyes and antibiotic," *Journal of Physics and Chemistry of Solids*, vol. 160, p. 110353, 2022.

[8] K. Alamelu and B. M. J. Ali, "Au nanoparticles decorated sulfonated graphene-TiO2 nanocomposite for sunlight driven photocatalytic degradation of recalcitrant compound," *Solar energy*, vol. 211, pp. 1194–1205, 2020.

[9] S. Alahiane, A. Sennaoui, F. Sakr, M. Dinne, S. Qourzal, and A. Assabbane, "Synchronous role of coupled adsorption-photocatalytic degradation of Direct Red 80 with nanocrystalline TiO2-coated non-woven fibres materials in a static batch photoreactor," *Groundw. Sustain. Dev.*, vol. 11, p. 100396, 2020.

[10] Y. Xiang, M. Gao, T. Shen, G. Cao, B. Zhao, and S. Guo, "Comparative study of three novel organo-clays modified with imidazolium-based gemini surfactant on adsorption for bromophenol blue," *J. Mol. Liq.*, vol. 286, p. 110928, 2019.

[11] J. Chen, Y. Pu, C. Wang, J. Han, Y. Zhong, and K. Liu, "Synthesis of a novel nanosilica-supported poly β-cyclodextrin sorbent and its properties for the removal of dyes from aqueous solution," *Colloids Surf. A Physicochem. Eng. Asp.*, vol. 538, pp. 808–817, 2018.

[12] S. Mishra, S. S. Sahoo, A. K. Debnath, K. P. Muthe, N. Das, and P. Parhi, "Cobalt ferrite nanoparticles prepared by microwave hydrothermal synthesis and adsorption efficiency for organic dyes: Isotherms, thermodynamics and kinetic studies," *Advanced Powder Technology*, vol. 31, no. 11, pp. 4552–4562, 2020.

[13] A. S. Shair, A. S. A. Dena, and I. M. El-Sherbiny, "Matrix-dispersed PEI-coated SPIONs for fast and efficient removal of anionic dyes from textile wastewater samples: Applications to triphenylmethanes," *Spectrochim. Acta A Mol. Biomol. Spectrosc.*, vol. 249, p. 119301, 2021.

[14] I. Fatimah, E. Z. Pratiwi, and W. P. Wicaksono, "Synthesis of magnetic nanoparticles using Parkia speciosa Hassk pod extract and photocatalytic activity for Bromophenol blue degradation," *Egypt. J. Aquat. Res.*, vol. 46, no. 1, pp. 35–40, 2020.

[15] A. C. Khorasani and S. A. Shojaosadati, "Magnetic pectin-Chlorella vulgaris biosorbent for the adsorption of dyes," *J. Environ. Chem. Eng.*, vol. 7, no. 3, p. 103062, 2019.

[16] W. Xiao *et al.*, "Adsorption of organic dyes from wastewater by metal-doped porous carbon materials," *J. Clean. Prod.*, vol. 284, p. 124773, 2021.

[17] S. Kocaman, "Removal of methylene blue dye from aqueous solutions by adsorption on levulinic acid-modified natural shells," *Int. J. Phytoremediation*, vol. 22, no. 8, pp. 885–895, 2020.

[18] S. De Gisi, G. Lofrano, M. Grassi, and M. Notarnicola, "Characteristics and adsorption capacities of low-cost sorbents for wastewater treatment: A review," *Sustainable Materials and Technologies*, vol. 9, pp. 10–40, 2016.

[19] F. Çatlıoğlu *et al.*, "Preparation and application of Fe-modified banana peel in the adsorption of methylene blue: process optimization using response surface methodology," *Environ. Nanotechnol. Monit. Manag.*, vol. 16, p. 100517, 2021.

[20] B. R. Patra, S. Nanda, A. K. Dalai, and V. Meda, "Slow pyrolysis of agro-food wastes and physicochemical characterization of biofuel products," *Chemosphere*, vol. 285, p. 131431, 2021.

[21] S. S. Sahoo, V. K. Vijay, R. Chandra, and H. Kumar, "Production and characterization of biochar produced from slow pyrolysis of pigeon pea stalk and bamboo," *Clean. Eng. Technol.*, vol. 3, p. 100101, 2021.

[22] S. Naik, V. V Goud, P. K. Rout, K. Jacobson, and A. K. Dalai, "Characterization of Canadian biomass for alternative renewable biofuel," *Renew. Energy*, vol. 35, no. 8, pp. 1624–1631, 2010.

[23] V. T. Trinh *et al.*, "Phosphate adsorption by silver nanoparticles-loaded activated carbon derived from tea residue," *Sci. Rep.*, vol. 10, no. 1, p. 3634, 2020.

[24] P. J. Wibawa, M. Nur, M. Asy'ari, and H. Nur, "SEM, XRD and FTIR analyses of both ultrasonic and heat generated activated carbon black microstructures," *Heliyon*, vol. 6, no. 3, 2020.

[25] R. K. Mishra and K. Mohanty, "Pyrolysis of Manilkara zapota seeds over ZSM-5 to produce high-quality bio-oil and chemicals," *Fuel*, vol. 280, p. 118594, 2020.

[26] A. Sahoo, S. Kumar, and K. Mohanty, "A comprehensive characterization of non-edible lignocellulosic biomass to elucidate their biofuel production potential," *Biomass Convers. Biorefin.*, vol. 12, no. 11, pp. 5087–5103, 2022.

[27] H. M. Oo, P. Karin, N. Chollacoop, and K. Hanamura, "Physicochemical characterization of forest and sugarcane leaf combustion's particulate matters using electron microscopy, EDS, XRD and TGA," *Journal of Environmental Sciences*, vol. 99, pp. 296–310, 2021.

[28] X. Yao, H. Zhou, K. Xu, Q. Xu, and L. Li, "Evaluation of the fusion and agglomeration properties of ashes from combustion of biomass, coal and their mixtures and the effects of K2CO3 additives," *Fuel*, vol. 255, p. 115829, 2019.

[29] S. M. A. El-Gamal, M. S. Amin, and M. A. Ahmed, "Removal of methyl orange and bromophenol blue dyes from aqueous solution using Sorel's cement nanoparticles," *J. Environ. Chem. Eng.*, vol. 3, no. 3, pp. 1702–1712, 2015.

[30] M. Ghaedi, A. M. Ghaedi, E. Negintaji, A. Ansari, A. Vafaei, and M. Rajabi, "Random forest model for removal of bromophenol blue using activated carbon obtained from Astragalus bisulcatus tree," *Journal of Industrial and Engineering Chemistry*, vol. 20, no. 4, pp. 1793–1803, 2014.

[31] H. Khoshsang, A. Ghaffarinejad, H. Kazemi, Y. Wang, and H. Arandiyan, "One-pot synthesis of S-doped Fe2O3/C magnetic nanocomposite as an adsorbent for anionic dye removal: equilibrium and kinetic studies," *J. Nanostructure Chem.*, vol. 8, no. 1, pp. 23–32, 2018.

[32] Y. Dehmani, A. A. Alrashdi, H. Lgaz, T. Lamhasni, S. Abouarnadasse, and I.-M. Chung, "Removal of phenol from aqueous solution by adsorption onto hematite (α-Fe2O3): Mechanism exploration from both experimental and theoretical studies," *Arabian Journal of Chemistry*, vol. 13, no. 5, pp. 5474–5486, 2020.

[33] Sali Mouhamadou, Constant Tcheka, Raphael Djakba, Narcisse Dobe, Gilbert Mando, and Massai Harouna, "INVESTIGATION OF Cr (VI) IONS ADSORPTIVE REMOVAL FROM AQUEOUS SOLUTION ONTO TiO2-AC COMPOSITE: NON-LINEAR EQUILIBRIUM MODELING AND KINETICS.," *Int. J. Eng. Sci. Res. Technol.*, vol. 10, no. 1, pp. 41–54, 2021, doi: 10.29121/ijesrt.v10.i1.2021.3.

[34] W. J. Weber Jr and J. C. Morris, "Kinetics of adsorption on carbon from solution," *Journal of the sanitary engineering division*, vol. 89, no. 2, pp. 31–59, 1963.

[35] I. Langmuir, "The adsorption of gases on plane surfaces of glass, mica and platinum.," *J. Am. Chem. Soc.*, vol. 40, no. 9, pp. 1361–1403, 1918.

[36] H. M. F. Freundlich, "Uber die adsorption in losungen," 1906.

[37] M. M. Dubinin, "The equation of the characteristic curve of activated charcoal," in *Dokl. Akad. Nauk. SSSR.*, 1947, pp. 327–329.

[38] M. K. David, U. C. Okoro, K. G. Akpomie, C. Okey, and H. O. Oluwasola, "Thermal and hydrothermal alkaline modification of kaolin for the adsorptive removal of lead (II) ions from aqueous solution," *SN Appl. Sci.*, vol. 2, no. 6, p. 1134, 2020.

[39] A. Q. Alorabi, M. S. Hassan, and M. Azizi, "Fe3O4-CuO-activated carbon composite as an efficient adsorbent for bromophenol blue dye removal from aqueous solutions," *Arabian Journal of Chemistry*, vol. 13, no. 11, pp. 8080–8091, 2020.

[40] K. G. Akpomie, S. Ghosh, M. Gryzenhout, and J. Conradie, "One-pot synthesis of zinc oxide nanoparticles via chemical precipitation for bromophenol blue adsorption and the antifungal activity against filamentous fungi," *Sci. Rep.*, vol. 11, no. 1, p. 8305, 2021.

[41] S. Dhananasekaran, R. Palanivel, and S. Pappu, "Adsorption of methylene blue, bromophenol blue, and coomassie brilliant blue by α-chitin nanoparticles," *J. Adv. Res.*, vol. 7, no. 1, pp. 113–124, 2016.

[42] M. Fathy, T. A. Moghny, M. A. Mousa, O. H. Abdelraheem, and A. A. Emam, "Synthesis and study bromophenol blue dye adsorption efficiency of reduced graphene oxide produced by catalytic acid spray (CAS) method," *Journal of the Australian Ceramic Society*, vol. 56, no. 2, pp. 567–577, 2020.

[43] M. B. Chabalala, M. Z. Al-Abri, B. B. Mamba, and E. N. Nxumalo, "Mechanistic aspects for the enhanced adsorption of bromophenol blue and atrazine over cyclodextrin modified polyacrylonitrile nanofiber membranes," *Chemical Engineering Research and Design*, vol. 169, pp. 19–32, 2021.

[44] J. M. Jabar, I. A. Owokotomo, Y. T. Ayinde, A. M. Alafabusuyi, G. O. Olagunju, and V. O. Mobolaji, "Characterization of prepared eco-friendly biochar from almond (Terminalia catappa L) leaf for sequestration of bromophenol blue (BPB) from aqueous solution," *Carbon Letters*, vol. 31, no. 5, pp. 1001–1014, 2021.

[45] B. Naceur, E. Abdelkader, L. Nadjia, and S. Esmahene, "NZF nanoscale particles: Synthesis, characterization and its effective adsorption of bromophenol blue," *Bulletin of Chemical Reaction Engineering & Catalysis*, vol. 15, no. 3, pp. 726–742, 2020.

[46] K. G. Akpomie, S. Ghosh, M. Gryzenhout, and J. Conradie, "One-pot synthesis of zinc oxide nanoparticles via chemical precipitation for bromophenol blue adsorption and the antifungal activity against filamentous fungi," *Sci. Rep.*, vol. 11, no. 1, p. 8305, 2021.

[47] P. R. De Souza, T. M. do Carmo Ribeiro, A. P. Lôbo, M. S. Tokumoto, R. M. De Jesus, and I. P. Lôbo, "Removal of bromophenol blue anionic dye from water using a modified exuviae of Hermetia illucens larvae as biosorbent," *Environ. Monit. Assess.*, vol. 192, no. 3, p. 197, 2020.